OPEN ACCESS

University of BRISTOL

Peer reviewed version

Link to published version (if available):
10.2514/6.2021-1266

Link to publication record in Explore Bristol Research
PDF-document

University of Bristol - Explore Bristol Research
General rights

Towards development of a nonlinear and flexible multi-body helicopter inceptor model: a resonant frequency tuning study.

E. J. H. Yap*[1], D. Rezgui*[2], M. H. Lowenberg*[3], S. A. Neild*[4]
University of Bristol, Bristol, BS8 1TR, United Kingdom

A. K. Rahman*[5]
BAE Systems, Rochester, Kent, ME1 2XX, United Kingdom

This paper presents an investigation into the mathematical modelling of the dynamics of a generic candidate inceptor mechanism when system linkage flexibilities are represented. The lumped parameter approach for modelling the flexibility is proposed and applied within the multi-body dynamic modelling framework formulated by Udwadia-Kalaba to explore system resonances. A low-order multi-body mathematical model of an inceptor system is derived and frequency response characteristics numerically obtained. Through a parametric design study, results show how resonance frequencies can be tuned to meet specified levels by identifying and recommending modifications in system design configurations at early design stages. The work presented in this paper provides a framework to identify acceptable design configurations of a system and offers parametric design insights within a multi-body dynamic environment.

I. Nomenclature

CG	=	Centre of Gravity
DoF	=	Degree of Freedom
E	=	Elastic Modulus
FEA	=	Finite Element Analysis
FE	=	Finite Element
FR	=	Frequency response
g	=	Gravity
I	=	Area moment of inertia
MAC	=	Modal Assurance Criterion
MBD	=	Multi-Body Dynamic
m	=	Mass
ODE	=	Ordinary Differential Equation
SAU	=	Servo Actuator Gearbox
U-K	=	Udwadia-Kalaba

*[1] Aerospace Engineering PhD student, Department of Aerospace Engineering, Student Member AIAA
*[2] Senior Lecturer in Aerospace Engineering, Department of Aerospace Engineering
*[3] Professor of Flight Dynamics, Department of Aerospace Engineering, Senior Member AIAA
*[4] Professor in Nonlinear Structural Dynamics, Department of Civil Engineering
*[5] Principal Mechanical Analysis Engineer, Electronic Systems

II. Introduction

Inceptors are the controls pilots use to manoeuvre and orientate an aircraft, applicable to both fixed and rotary wing aircraft. Inceptors, whilst commonly referred to as 'sticks', comprise an entire class of pilot interface controls that range from centre sticks, side sticks, cyclics to throttle controls. An active inceptor includes the unique ability to provide tactile force feedback from the aircraft control surfaces to the pilot; this provides valuable input- response cues to the pilot and can thereby improve aircraft handling qualities. Examples of aircraft active inceptor systems are shown in Fig. 1.Whilst active inceptors have predominantly been reserved for military applications [1] there have been increasing efforts to incorporate active inceptors within the civilian aviation sector fuelled by some notable high profile events [2].

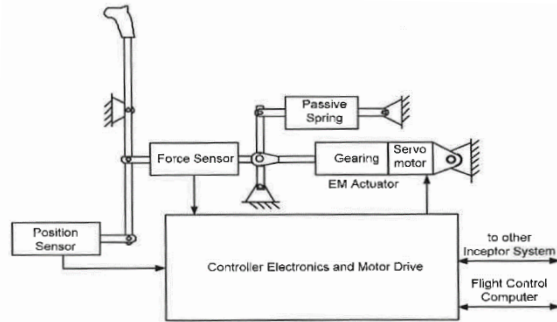**Fig. 1 Aircraft inceptor control systems [3]**

Fig. 2 Functional block diagram schematic of an active inceptor [4]

The unique functionality of active inceptors providing tactile force feedback to the pilot means their anatomies typically comprise combinations of linear and torsional springs, motors, servo actuators, ball bearings, spherical bearings and displacement and force transducers [4]. These components are all interconnected through a network of mechanical linkages which the functional block diagram schematic in Fig. 2 encapsulates for a generic active inceptor system. In the design for vibrations, it is crucial to understand how these individual components collectively behave under the influence of helicopter vibratory loads. For structures within a helicopter chassis, rotor vibratory loads are considered the key driver [5] and some inceptor system resonances may possibly coincide or occur near the forcing frequencies of the aircraft. It is imperative that this is avoided.

In early industrial design stages, an active inceptor's dynamic characteristics and performance may not be adequately predited nor assessed due to the nature of system design being in a continual state of change, further complicated by the nonlinearity and uncertainty of various joints and actuation systems. The use of refined finite element analyses to assess the full system's dynamic behaviour may not be efficient until the inceptor design has passed into the detailed design stage since it offers little parametric design insight [6]. However if significant issues do emerge once the inceptor design is finalised, such as system component resonances occurring close to or at the forcing frequencies of the target aircraft, then the inceptor design may be subjected to an undefined number of design iterations to ensure sufficient clearance is observed. The target aircraft's forcing frequencies will be dominated by rotating components such as the main or tail rotor as specified by MIL-STD 810G [5]. However, there is no assurance that further design iterations in the system design will not lead to an inadvertent shift of additional inceptor component resonances to now occur near the aforementioned aircraft forcing frequencies. The potential reactive nature of inceptor design iterations that may ensue, coupled with adverse impacts on project time scales, often leads to a general reluctance within industry to substantially alter an inceptor design upon its initial finalisation.

The prospect for an undefined number of inceptor iterative design cycles to mitigate the proximity and potential overlap of inceptor system resonances with the target aircraft forcing frequencies motivates the need to develop an efficiently configurable *reduced-order* mathematical model of a candidate active inceptor that offers parametric design insights and studies. The mathematical model would be used to provide an early low-cost means of predicting the dynamics of the inceptor mechanism in preliminary design stages to and through frequency response analyses, pre-empt the occurrence of adverse vibration issues. Inceptor resonant frequencies may be identified and tuned to levels that comply with specified frequency restrictions by identifying the required modifications to the inceptor system design configuration in early design stages.
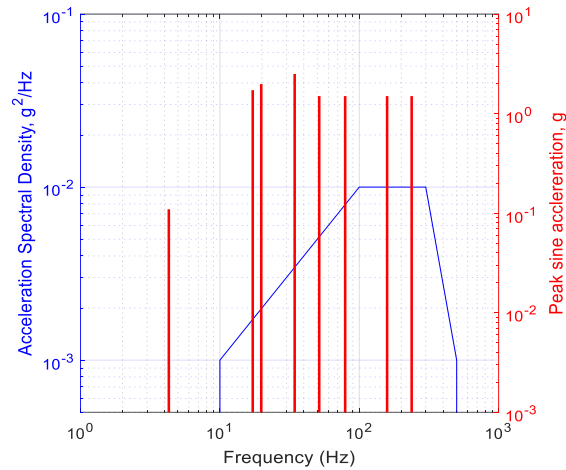

Fig. 3 Example 'Sine on Random' vibration profile for a UH-60 Helicopter [7]

'Sine on Random' is a specific class of vibration profile used for vibration qualification testing of helicopter internally stored cargo as specified within MIL-STD 810G [5]. Sine on Random vibration profiles, as shown in Fig. 3, are unique as they comprise strong narrowband sinusoidal vibration peaks from rotating components of the helicopter (predominantly from the main and tail rotors) superimposed over low-level wideband random aerodynamic flow vibration. The intention of such a profile is to simulate the worst-case environments that helicopter internally stored cargo may be subjected to throughout their lifetime and to effectively determine the frequency avoidance regions for resonant frequencies of components to coincide.

The inceptor system is an example of a multi-body system comprising components characterised by kinematic nonlinearity that can endure significant displacements and bodies interconnected through joints. This highlights the importance of investigating Multi-Body Dynamic (MBD) modelling approaches in order to mathematically model the system's dynamic behaviour in regard to resonance frequencies with appropriate accuracy. Section III provides a brief summary of the proposed MBD modelling methodology for use in this work, formulated by Udwadia-Kalaba [8] (U-K). This modelling approach is proposed as it specifically addresses the modelling of multibody mechanical systems subjected to kinematical constraints. The solution techniques are efficient [9] since the formulations result in a system of Ordinary Differential Equations (ODEs) that may be solved using standard explicit time integration solvers. The formulations also eliminate the use of Lagrange multipliers [9] which are often difficult to obtain for systems with a large number of degree of freedoms (DoFs) [10].

Previous formulations of constrained system motion have been proposed, such as by Gibbs and Appell, Gauss and Hamilton; however the Udwadia-Kalaba formulations have the benefit of providing an explicit set of equations for general constrained systems [10]. Whilst MBD applications are available such as provided by MSC Adams [11] and Dymore [12], the overriding intention of this work is to develop a *reduced-order*, low cost model of a multibody inceptor system to aid its dynamic analysis and offer parametric design insight in preliminary design stages. This provides the rationale for adopting the Udwadia-Kalaba formulations for this work.

This paper shows how system natural frequencies for a nonlinear and flexible candidate inceptor system can be identified and tuned within the MBD framework formulated by Udwadia-Kalaba. The dynamics of flexibility of selected components within the inceptor system are idealised through the incorporation of linkage compliance using a lumped parameter approach. The contribution of this paper is to offer parametric design insight of the nonlinear and flexible candidate inceptor system at early design stages by using a *reduced-order* mathematical model to inform necessary modifications in system configurations to comply with specified frequency restrictions.

The following section provides a brief outline of the Udwadia-Kalaba MBD modelling approach. Section IV demonstrates the adaptation of the Udwadia-Kalaba approach to model flexible bodies. An application study is also presented of modelling a flexible beam using the lumped parameter approach within the Udwadia-Kalaba framework. Section V then addresses the modelling of the nonlinear and flexible candidate inceptor system and the parametric design studies that ensue.

III.   The Udwadia-Kalaba MBD modelling approach

The Udwadia-Kalaba [8] equations of motion as presented in Eq. (1) are proposed for use in this work as they specifically address the modelling of multi-body mechanical systems subjected to kinematical constraints. The formulations place heavy emphasis on the derivation of the system's constraint equations and reduce the system to a corresponding system of rigid bodies with the system's physical geometrical constraints included as a separate entity.

$$\ddot{\mathbf{x}} = \mathbf{a} + M^{-\frac{1}{2}}\left(AM^{-\frac{1}{2}}\right)^{+}(\boldsymbol{b} - A\mathbf{a}) \tag{1}$$

$\ddot{\mathbf{x}}$ is the vector of true accelerations of the multibody system that includes the influence of applied geometric constraints. $\mathbf{a}$ refers to the vector of external accelerations due to impressed forces acting on the system with size (q x 1) where q denotes the number of system state variables. M is the mass matrix of the system, of size (q x q). The + symbol represents the Moore-Penrose generalized pseudoinverse function [13]. The Udwadia-Kalaba formulations assume that the set of constraint equations derived for generic systems may be expressed in the form of Eq.(2), as linear equality relations regarding accelerations between the rigid bodies of the system.

$$A\ddot{\mathbf{x}} = \boldsymbol{b} \tag{2}$$

A is a matrix of size (p x q) with terms associated with state accelerations obtained from the differentiation of the system's geometric constraint equations twice with respect to time and formulated in the form of Eq. (2). The quantity p refers to the number of geometric constraint equations derived for the system. $\boldsymbol{b}$ is a vector of size (p x 1) populated with terms that are not associated with state accelerations when the geometric constraint equations are differentiated twice with respect to time and expressed in the form of Eq. (2).

Considering Eq. (1), the right hand side terms consisting of $M^{-\frac{1}{2}}\left(AM^{-\frac{1}{2}}\right)^{+}(\boldsymbol{b} - A\mathbf{a})$ represent the additional acceleration constraints brought into play to ensure that the system satisfies the geometric constraints it is subjected to. This dynamic modelling approach has also previously been investigated by Nielsen et al [14], Li et al [15] and Xu et al [16] who all found convincing agreement of simulated system dynamic results with reference data. In 2019, previous work of the authors [7] provided an application study of the Udwadia-Kalaba modelling approach to a rigid nonlinear planar crank-slider linkage mechanism. The dynamic behaviour of the mechanism under the influence of an externally applied sinusoidal force was assessed with results shown to match responses from alternatively-formulated models produced within MATLAB's MBD toolkit Simscape [17] and a reduced coordinate Lagrangian method. Results from the study validated the system responses produced from the Udwadia-Kalaba modelling approach against the other modelling methods [7] and demonstrated the applicability of the Udwadia-Kalaba modelling approach to dynamically model generic multibody systems subjected to kinematical constraints that may also display nonlinearity. In the aforementioned studies, the application of the Udwadia-Kalaba modelling approach was limited to rigid-body systems. This paper extends the application of this modelling approach to consider the inherent flexibility of multibody systems by considering components as being deformable.

The Udwadia-Kalaba formulations were also compared against alternative modelling methodologies [10], however it was observed that this modelling approach provided for the first time an explicit set of equations for general constrained systems. The equations of motion obtained may be numerically solved, requiring only the system's mass matrix, acceleration vector due to impressed forces and geometric constraint equations expressed as ordinary differential equations.

IV. Adaptation to modelling flexible systems within Udwadia-Kalaba approach

The underlying principle of the Udwadia-Kalaba formulation is to reduce the physical system to a corresponding system of rigid bodies with geometric constraint equations governing their relations. Therefore, in the extension to flexible multi-body systems, the lumped parameter approach is adopted within the Udwadia-Kalaba framework where flexible links are idealised as a series of rigid elements connected by a set of springs as illustrated in Fig. 4.
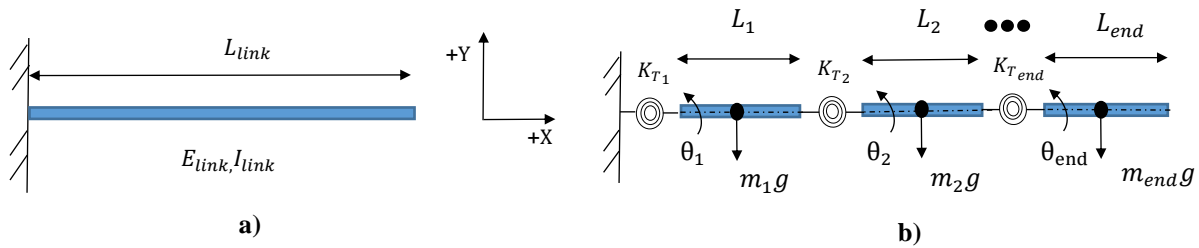

Fig. 4 a) Illustration of the flexible link b) lumped parameter representation of the flexible link into a series of rigid elements connected by springs

In Fig. 4a), L, E and I represent the length, elastic modulus and area moment of inertia of the respective link. Within the lumped parameter model of the flexible link in Fig. 4b), K_{T_i} denotes the stiffness of individual torsional springs, L_i denotes the length of individual rigid elements and m_i the mass of individual rigid elements. The acceleration due to gravity (g) and orientation of each individual rigid element relative to the global horizontal (θ_i) is also defined. An in-depth case study of a planar beam with free-free boundary conditions is now presented to demonstrate the application of the Udwadia-Kalaba approach in producing a lumped parameter model representation that accurately captures the dynamic behaviour of the original beam

A. Free-Free beam case study

In this case study a planar beam with free-free boundary conditions and rectangular cross section is considered. The beam is modelled in the absence of boundary conditions to represent modelling an isolated component. Beam properties are tabulated in Table. 1 and a finite element (FE) model of the beam produced within MSC Patran [18] is shown in Fig. 5. Views of the beam's first four mode shapes in the absence of boundary conditions in addition to the corresponding modal frequencies are also shown. For the purpose of this exercise in evaluating the Udwadia-Kalaba modelling, the FE model is regarded as a true representation of the beam, referred to below as the 'original beam'

Table. 1 Material and geometrical properties of the beam

Elastic Modulus (Gpa)		70
Density	(kgm^{-3})	2710
Poisson ratio		0.3
Length	(m)	$2\sqrt{2}$
Width	(m)	0.050
Height	(m)	0.0026

Mode 1 at 1.7039 Hz

Mode 2 at 4.6969 Hz

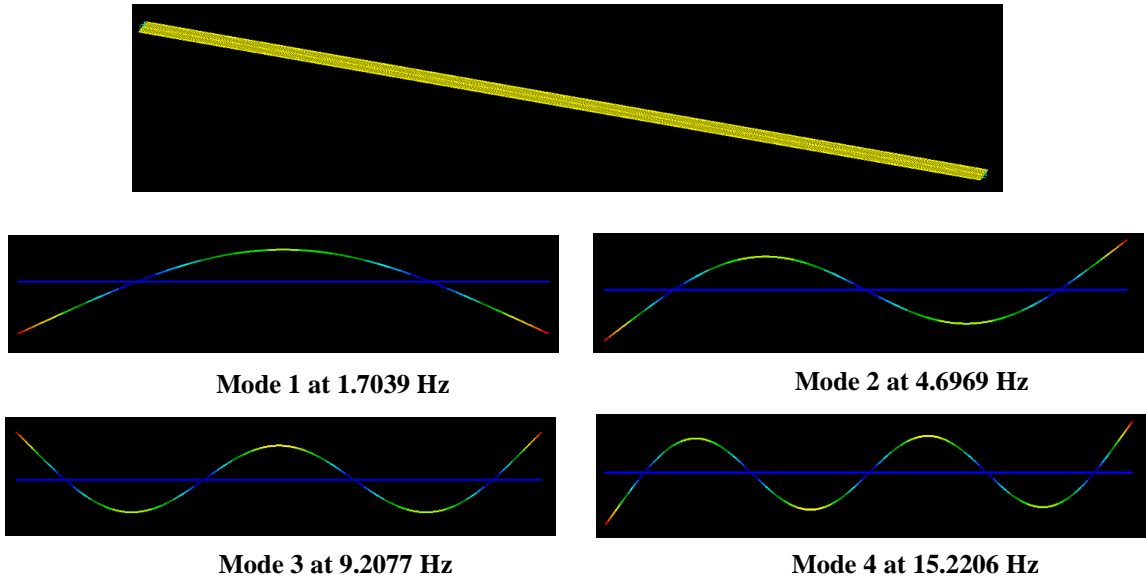**Mode 3 at 9.2077 Hz**

Mode 4 at 15.2206 Hz

Fig. 5 Finite element model representation of the beam with free-free boundary conditions and corresponding first four mode shapes with natural frequencies. Produced within MSC Patran.

FEA modal analysis was conducted to extract the original beam's natural frequencies and mode shapes. Only the first four beam modes are considered of interest. The lumped parameter beam model is required to accurately depict and capture the dynamic behaviour of the original beam and so the basis for determining appropriate mass and stiffness values was through comparing the dynamics of the discretised beam with the original beam modelled within FE. A set of criteria for the lumped parameter beam model to satisfy eight modal properties corresponding to the original beam was established. The first four criteria would correspond to ensuring a match with the four beam modal frequencies whilst the last four criteria correspond to ensuring a correlation with the original beam's four mode shapes. The original beam was accordingly discretised into nine uniform rigid elements interconnected by eight torsional springs as illustrated in Fig. 6.
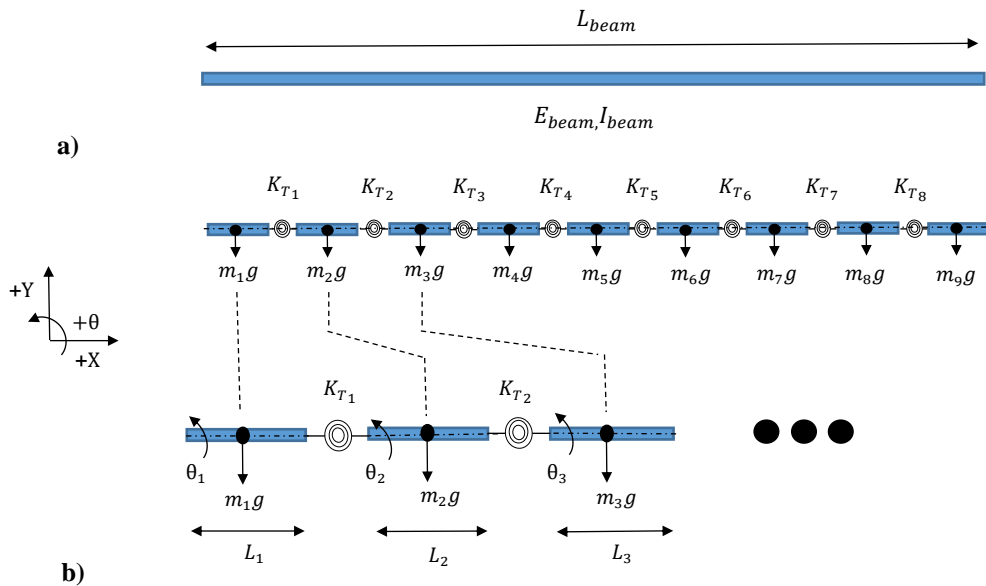

Fig. 6 a) Illustration of the original beam b) lumped parameter diagrammatic representation of the original beam

The Udwadia-Kalaba dynamic modelling approach places heavy emphasis on the derivation of the system's geometric constraint equations. For the lumped parameter beam model which discretised the original beam into nine uniform rigid elements, twenty-seven geometric position states (X_i, Y_i, θ_i for each rigid element) may be used to define the configuration of the system in space. X_i, Y_i denote rigid element centre of gravity (CG) translations and θ_i represents the element rotations relative to the horizontal. The geometric constraint equations governing the position of each rigid element in space is presented through Eqs. (3) to (18).

$$X_2 = X_1 + \frac{L_1}{2}\cos(\theta_1) + \frac{L_2}{2}\cos(\theta_2) \quad (3)$$

$$X_6 = X_5 + \frac{L_5}{2}\cos(\theta_5) + \frac{L_6}{2}\cos(\theta_6) \quad (11)$$

$$Y_2 = Y_1 + \frac{L_1}{2}\sin(\theta_1) + \frac{L_2}{2}\sin(\theta_2) \quad (4)$$

$$Y_6 = Y_5 + \frac{L_5}{2}\sin(\theta_5) + \frac{L_6}{2}\sin(\theta_6) \quad (12)$$

$$X_3 = X_2 + \frac{L_2}{2}\cos(\theta_2) + \frac{L_3}{2}\cos(\theta_3) \quad (5)$$

$$X_7 = X_6 + \frac{L_6}{2}\cos(\theta_6) + \frac{L_7}{2}\cos(\theta_7) \quad (13)$$

$$Y_3 = Y_2 + \frac{L_2}{2}\sin(\theta_2) + \frac{L_3}{2}\sin(\theta_3) \quad (6)$$

$$Y_7 = Y_6 + \frac{L_6}{2}\sin(\theta_6) + \frac{L_7}{2}\sin(\theta_7) \quad (14)$$

$$X_4 = X_3 + \frac{L_3}{2}\cos(\theta_3) + \frac{L_4}{2}\cos(\theta_4) \quad (7)$$

$$X_8 = X_7 + \frac{L_7}{2}\cos(\theta_7) + \frac{L_8}{2}\cos(\theta_8) \quad (15)$$

$$Y_4 = Y_3 + \frac{L_3}{2}\sin(\theta_3) + \frac{L_4}{2}\sin(\theta_4) \quad (8)$$

$$Y_8 = Y_7 + \frac{L_7}{2}\sin(\theta_7) + \frac{L_8}{2}\sin(\theta_8) \quad (16)$$

$$X_5 = X_4 + \frac{L_4}{2}\cos(\theta_4) + \frac{L_5}{2}\cos(\theta_5) \quad (9)$$

$$X_9 = X_8 + \frac{L_8}{2}\cos(\theta_8) + \frac{L_9}{2}\cos(\theta_9) \quad (17)$$

$$Y_5 = Y_4 + \frac{L_4}{2}\sin(\theta_4) + \frac{L_5}{2}\sin(\theta_5) \quad (10)$$

$$Y_9 = Y_8 + \frac{L_8}{2}\sin(\theta_8) + \frac{L_9}{2}\sin(\theta_9) \quad (18)$$

The above geometric constraint equations were formulated within MATLAB and in accordance with the process stipulated in Section III, the necessary A, M matrices and a, b vectors were obtained to construct the dynamic model of the system based on the Udwadia-Kalaba approach in Eq. (1).

The masses of individual rigid elements were determined through equivalating the geometrical and material properties of the original beam across the nine rigid elements. In order to determine individual torsional spring stiffnesses, an iterative backwards process was derived that involved evaluating the numerical modal frequencies and mode shapes of the lumped parameter beam model formulated within the Udwadia-Kalaba framework and comparing quantities against specified target modal frequencies and mode shapes of the original beam. MATLAB's in-built *numjac* and *fsolve* functions (version 2019a) were used to facilitate the process. A flow chart illustrating this process is presented in Fig. 7. MATLAB's *fsolve* function is a nonlinear system solver relying primarily on the *trust-region-dogleg* algorithm which requires the number of equations to be at least the same number of unknowns [19]. On the other hand, the *numjac* function numerically evaluates the Jacobian of a function, returning a matrix term [20].
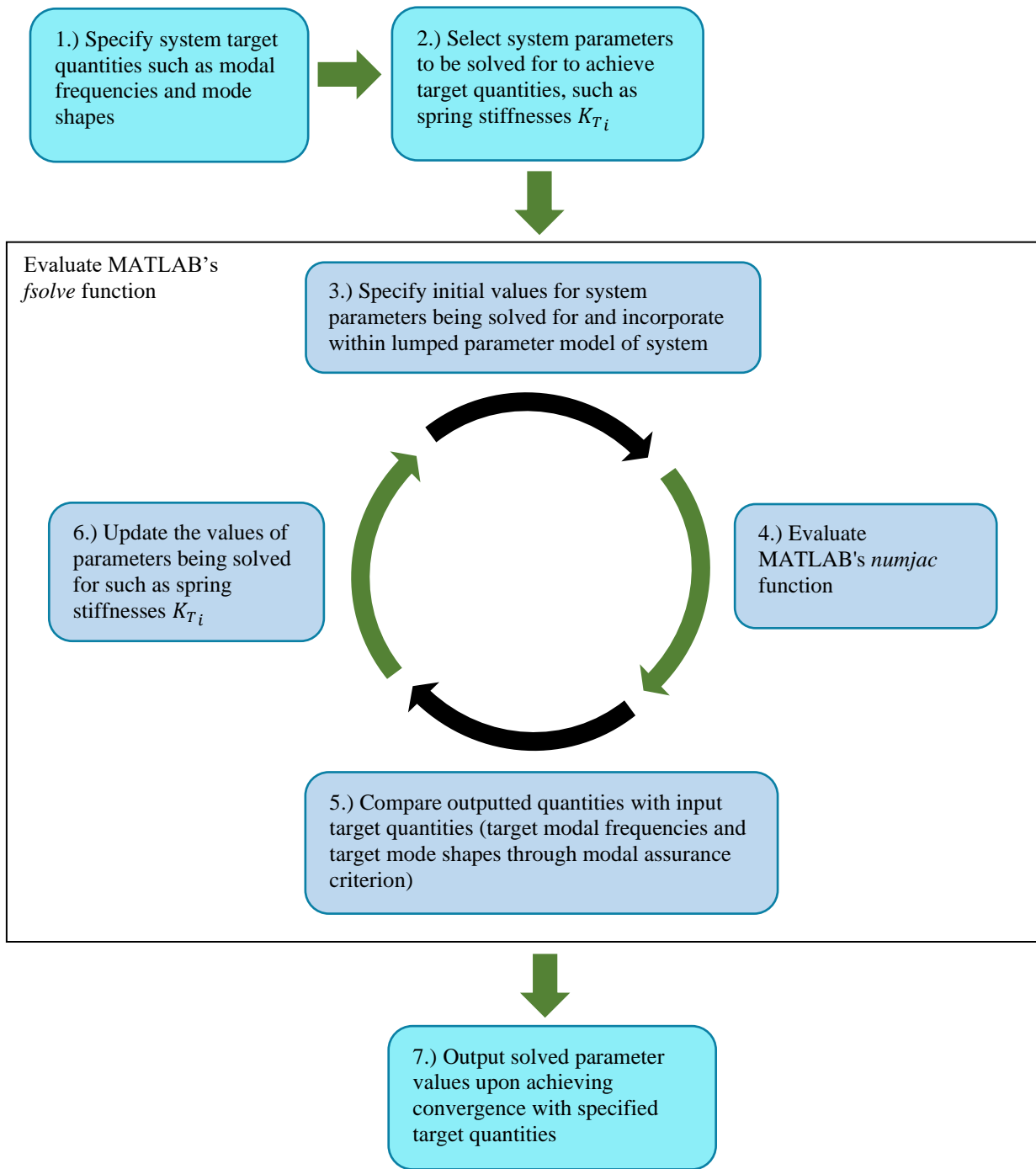
Fig. 7 Outlining the iterative backwards process

Table. 2 Lumped parameter model solved torsional spring stiffnesses

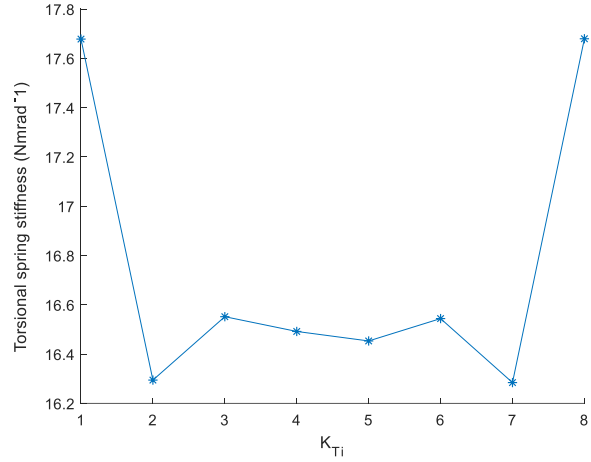| Torsional spring stiffnesses (Nmrad^{-1})	
K_{T_1}	17.6780
K_{T_2}	16.2943
K_{T_3}	16.5516
K_{T_4}	16.4916
K_{T_5}	16.4531
K_{T_6}	16.5439
K_{T_7}	16.2842
K_{T_8}	17.6793

Fig. 8 Lumped parameter model solved torsional spring stiffnesses

The resulting torsional spring stiffnesses outputted are presented in Table 2 and visualised in Fig. 8. Validation of the obtained torsional spring stiffnesses was performed through re-incorporating the stiffness values within the Udwadia-Kalaba lumped parameter beam model and numerically evaluating the system's numerical natural frequencies. Results are displayed in Table. 3. Comparisons were made with the beam's original modal frequencies extracted from FEA.

A comparison of the correlation of mode shapes with that of the original beam was also performed through the determination of the Modal Assurance Criterion (MAC) [21]. The MAC provides a measure to determine the degree of correlation between mode shapes from two different data sets. It is a scalar quantity defined by Eq. (19) [21]:

$$MAC(A,X) = \frac{|\{\psi_X\}^T\{\psi_A\}|^2}{(\{\psi_X\}^T\{\psi_X\}).(\{\psi_A\}^T\{\psi_A\})} \tag{19}$$

The terms A and X refer to the two different data sets being compared against with ψ_i denoting the mode shape quantity. The term T is the transpose function. The outputs of Eq. (19) are scalar quantities in between zero and one, with a value of close to one indicating a high degree of correlation between the modes being compared. Similarly, a MAC value close to zero signifies that the modes being compared are uncorrelated and indicates that they relate to two different modes. It is generally found that a MAC value in excess of 0.9 is obtained for well-correlated modes whilst values below 0.1 is indicative of uncorrelated modes [21]. The MAC values for the four modes are tabulated in Table. 3 and indicated in Fig. 9.

Table. 3 Comparison of modal frequencies and MAC

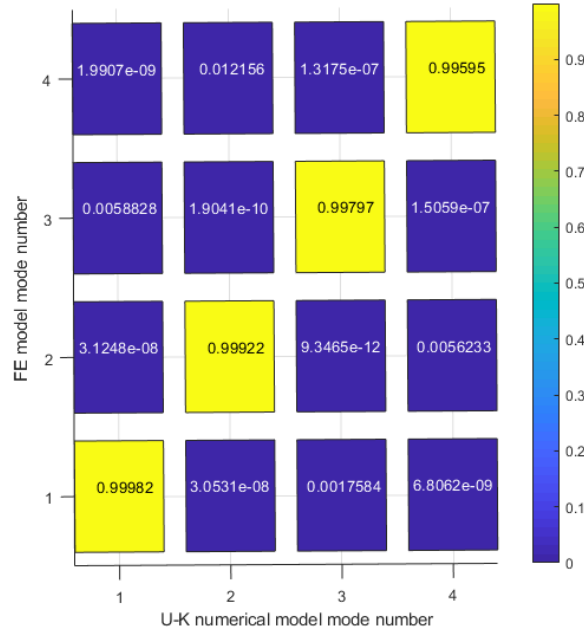| Mode Number	FE beam model frequencies, Hz	U-K beam model frequencies, Hz	MAC
1	1.704	1.704	0.99982
2	4.697	4.697	0.99922
3	9.208	9.208	0.99797
4	15.22	15.22	0.99595

Fig. 9 MAC plot showing correlation of modes of the beam with those numerically obtained through the Udwadia-Kalaba lumped parameter approach.

Results from Table. 3 show that the solved torsional spring stiffnesses in Table. 2 when incorporated within the lumped parameter beam model may successfully reobtain the original beam's modal frequencies. Additionally the high degree of correlation of numerical mode shapes with that of the original beam observed in Fig. 9 demonstrates not only the promising nature of the methodology in determining the lumped parameters of the discretised system but also the capability to adapt the Udwadia-Kalaba approach to represent the dynamic behaviour of flexible systems.

In a further assessment into the similarity of the lumped parameter beam model to that of the original beam, the influence of appending boundary conditions is now considered. The overriding motivation is to explore situations in which the beam's range of kinematic motion is now limited such as it being incorporated within a mechanical assembly. Since the resulting dynamic behaviour of the beam is directly influenced by the boundary conditions applied, the ability of the lumped parameter beam model to continue capturing and representing the dynamics of the beam under the influence of boundary conditions is now assessed

1. Assessment of the influence of changing the boundary conditions to Pinned-Free

The original beam was constrained at its root with a pin joint and its dynamic behaviour explored. The lumped parameter beam model formulated within the Udwadia-Kalaba framework was modified simply through appending two additional geometric constraints, equations Eq. (20) and (21), to represent the application of the root pin joint. The originally solved lumped mass and stiffness parameters were retained.

$$X_1 = \frac{L_1}{2} \cos(\theta_1) \qquad (20)$$

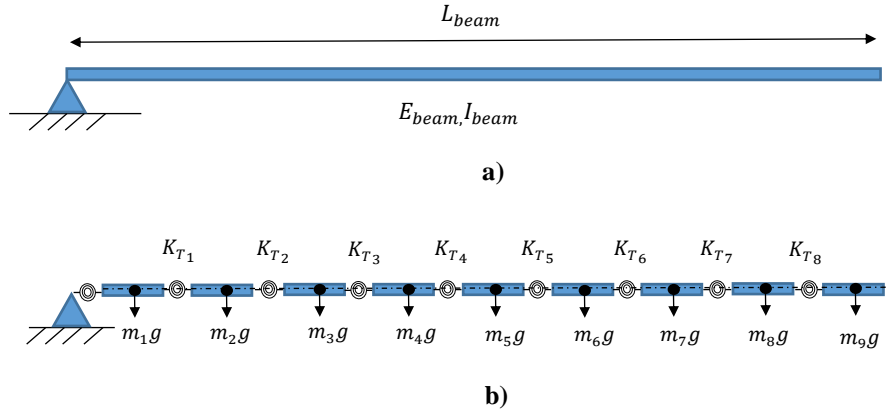$$Y_1 = \frac{L_1}{2} \sin(\theta_1) \qquad (21)$$

10

Fig. 10 a) Illustration of the beam with pinned-free boundary conditions b) lumped parameter diagrammatic representation of the beam with pinned-free boundary conditions.

Figure. 10 illustrates the beam modified with a pinned-free boundary condition and the corresponding lumped parameter model representation. FE modal analysis was conducted to extract the modal frequencies and mode shapes of the beam with a pinned boundary condition at the root. Comparisons of the beam's dynamic behaviour were then made with those from the lumped parameter Udwadia-Kalaba representation in Table. 4.

Table. 4 Comparison of modal frequencies and MAC

Mode Number	FE beam model frequencies with pinned-free boundary conditions, Hz	U-K beam model frequencies with pinned-free boundary conditions, Hz*	Percentage difference, %		MAC
1	1.174	1.175	0.09		0.99993
2	3.805	3.814	0.24		0.99964
3	7.939	7.976	0.47		0.99896
4	13.58	13.65	0.52		0.99804

* Using the torsional spring stiffnesses computed in Table. 2

Results from Table. 4 comparing modal frequencies in addition to the MAC reveal a very strong match and respective correlation of data. The results show that by simply appending Eqs. (20) and (21) within the Udwadia-Kalaba lumped parameter model whilst retaining the originally solved lumped parameters, the maximum discrepancy in modal frequency is 0.52%. The recorded MAC quantities in Table. 4 are still in excess of 0.9 which further demonstrates the continued representative depiction of the constrained beam using the lumped parameter approach within the Udwadia-Kalaba framework.

2. Assessment of the influence of changing the boundary conditions to Pinned-Pinned with translational freedom

A final assessment was performed by overlaying an additional boundary condition to the beam at its end. The end of the beam was now to be attached to the ground through a translational-revolute joint, resulting a beam with a pinned-pinned with translation boundary condition as illustrated in Fig. 11.

11
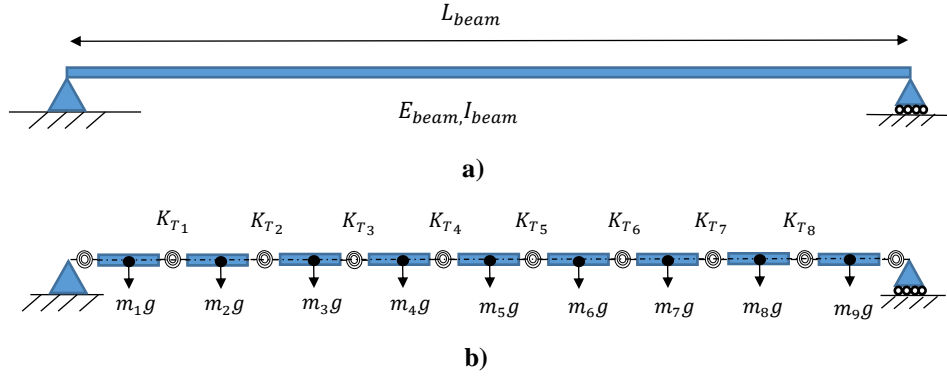
Fig. 11 a) Illustration of the beam with a pinned-pinned with translational boundary condition
b) lumped parameter diagrammatic representation of the beam with pinned-pinned with translational boundary conditions.

The attachment of the beam end to the ground through a translational-revolute joint within the Udwadia-Kalaba lumped parameter model was captured by appending a single additional constraint, equation Eq. (22)

$$Y_9 = -\frac{L_9}{2}\sin(\theta_9) \qquad (22)$$

FE modal analysis was conducted to extract the modal properties of this constrained beam with results compared against those from the lumped parameter representation in Table. 5.

Table. 5 Comparison of modal frequencies and MAC

Mode Number	FE beam model frequencies with pinned-pinned with translation boundary conditions, Hz	U-K beam model frequencies with pinned-pinned with translation boundary conditions, Hz*	Percentage difference, %		MAC
1	0.7517	0.7525	0.11		0.99999
2	3.007	3.019	0.40		0.99994
3	6.765	6.820	0.81		0.99978
4	12.03	12.16	1.08		0.99961

* Using the torsional spring stiffnesses computed in Table. 2

A comparison of modal frequencies as shown in Table. 5 between the Udwadia-Kalaba lumped parameter beam model and FE beam model reveal a maximum discrepancy of 1.08% for the modes considered. This in addition to the high correlation of MAC provide further reassurance that the lumped parameter beam is successfully capturing the dynamics of the original beam with constrained boundary conditions.

The underlying findings of the presented case study which conjunctively highlights its motivational purpose shows that flexible systems regardless of applied boundary conditions may be represented using the lumped parameter approach so long as respective constraint equations are derived and systematically appended within the Udwadia-Kalaba framework. The originally solved lumped parameters (in the form of masses and spring stiffnesses in this case study) need not be modified or altered. Extending the application of the Udwadia-Kalaba methodology to model flexible systems using the lumped parameter approach has shown to be a promising framework to adopt. Results have shown to be able to successfully capture the dynamic behaviour of the original flexible system. This modelling framework is now carried forward to the nonlinear and flexible candidate inceptor system to explore its dynamic characteristics.

V. The candidate inceptor system

The candidate inceptor is a helicopter active collective stick unit. Helicopter collective sticks are responsible for dictating the levels of vertical lift generated by the main rotor blades by governing their pitch angle collectively. This work will only consider the modelling of the inceptor mechanism housed within the chassis. A simplified description of central components within the inceptor mechanism and their connections is now detailed. The mechanism is three-dimensional and components of interest include the control stick which protrudes out of the external chassis and provides the interface between the subject pilot and inceptor mechanism. The end of the control stick bridging into the inceptor chassis is pivoted and attached to a servo actuator gearbox (SAU). This SAU is attached rigidly to a crank arm link via an out-of-plane rotating shaft element. The end of the crank arm link is then connected to a force sensor element which itself is mounted to the chassis port-side wall at its other end. This information is summarised in the functional block schematic in Fig. 12 and visually illustrated in Fig. 13. In 2019, previous work of the authors [7] investigated using the Udwadia-Kalaba modelling approach to mathematically model a nonlinear rigid candidate inceptor mechanism to explore resonance frequencies. The ensuing phase addressed here is the increasing of model complexity by representing the dynamics of flexibility in selected components through incorporating linkage flexibilities.
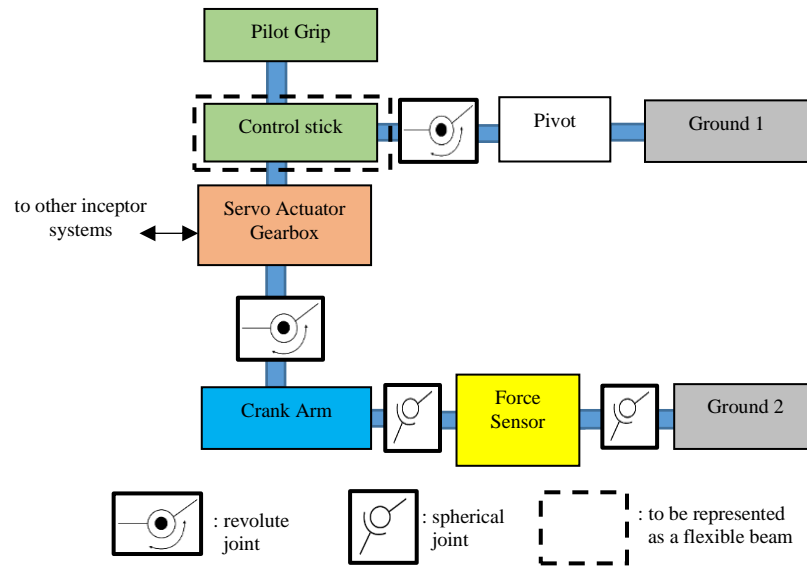

Fig. 12 Functional block diagram schematic of the candidate inceptor outlining component connection sequence
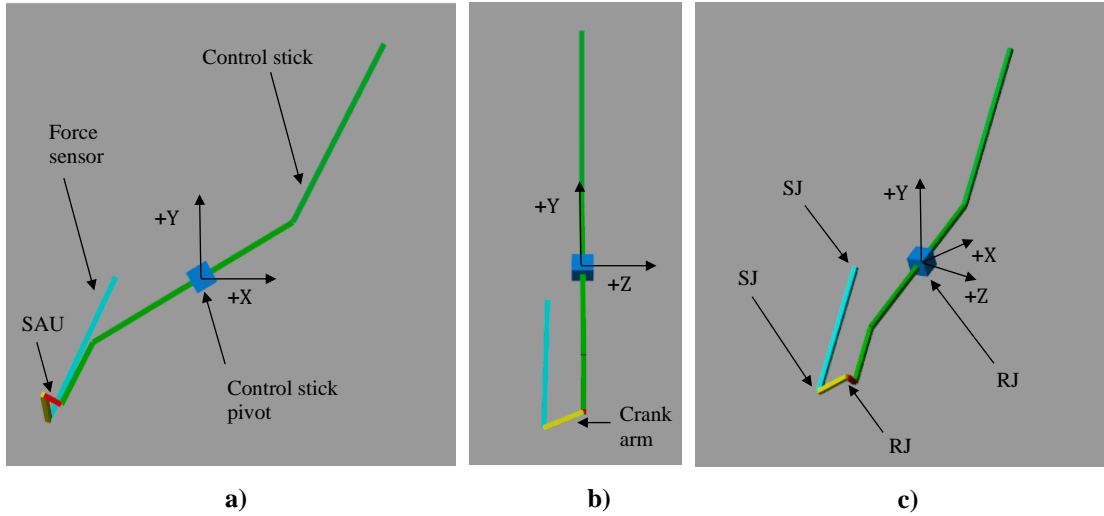
Fig. 13 MATLAB Simscape kinematical model of the inceptor mechanism.
SJ refers to a spherical joint. RJ refers to a revolute joint.

Figure. 13 is a reduced representation of the inceptor mechanism produced within MATLAB Simscape to illustrate the kinematical behaviour of the mechanism. The model provides further visualisation of the mechanism's central components and connections outlined in Fig. 12. In Fig. 13, the series of green links represent the inceptor control stick. The SAU is represented by the red link and the crank arm represented by the yellow link. The end of the crank arm is connected to the force sensor element which is represented by the cyan link.

The inceptor control stick due to its geometry and inherent flexibility is to be considered deformable through linkage flexibilities as schematically shown in Fig. 12. For this work, only the in-plane fore-aft bending flexible modes of the inceptor control stick are considered of interest which in Fig. 13 corresponds to the X-Y plane. Lateral flexible modes are ignored. The flexibility is idealised through lumped parameters within the Udwadia-Kalaba framework which has been shown (in section III and IV) to be applicable for generic multibody systems subjected to kinematical constraints.

B. Lumped parameter representation of the inceptor stick.

To idealise the inceptor control stick using the lumped parameter approach and to determine the suitable number of rigid elements to represent it, the control stick was firstly isolated from the inceptor system unit. In the absence of any boundary condition constraints, an FE analysis was conducted on the control stick to extract its modal properties. A conservative frequency search range spanning 0-500 Hz was defined in which a single flexible fore-aft bending mode was recorded at 278.58 Hz.

The lumped parameter model of the inceptor stick was formulated by defining the criteria that it should satisfy the modal frequency and mode shape of the recorded flexible mode. Therefore, the minimum number of rigid elements that would be required to represent the dynamics of the flexible inceptor control stick is three: this is the case considered here. The three rigid elements would be interconnected via two torsional springs initially of unknown spring stiffnesses. This is summarised in Fig. 14.
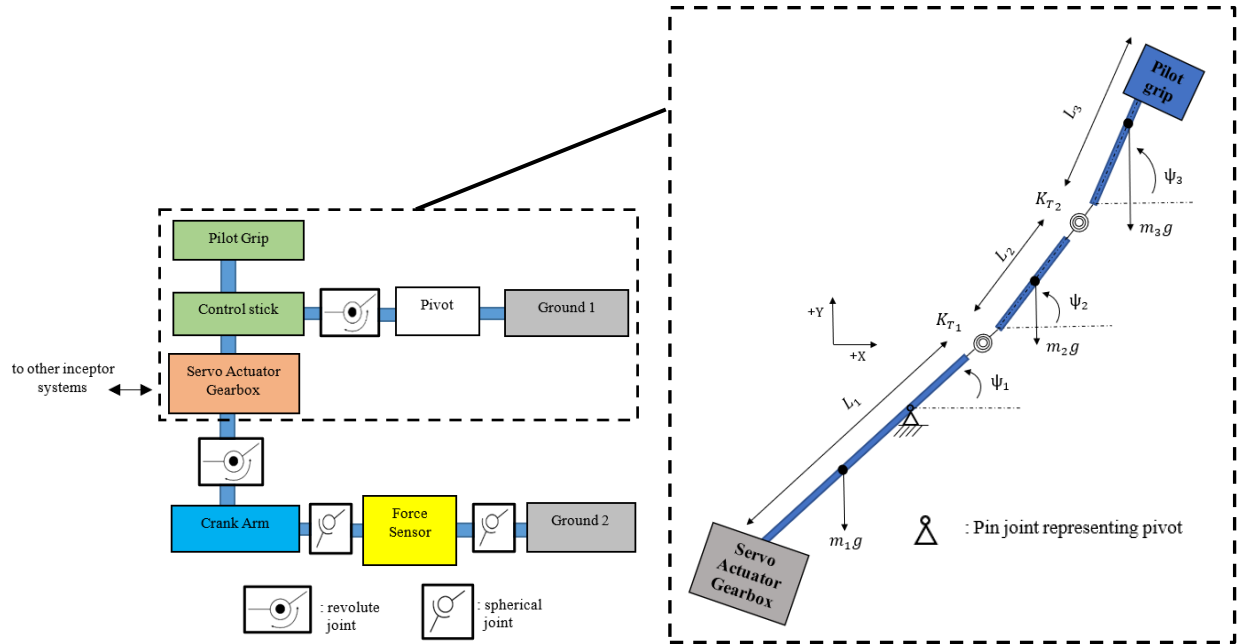
Fig. 14 Idealising the flexible inceptor control stick through the lumped parameter approach

To determine the locations at which to partition the inceptor stick into three rigid elements, the mode shape of the inceptor control stick's flexible mode was inspected within FEA. The deformed view of the control stick provided information to establish the approximate location of where to place each rigid element under the lumped parameter approach. Values for individual rigid element lumped masses and mass moment of inertias were extracted from the inceptor control stick FE model by considering the three unique partitions of the control stick. To determine individual spring torsional stiffnesses in Fig. 14, the iterative backwards process outlined in Section IV was used. The numerical modal frequency and mode shape of the lumped parameter model formulated within the Udwadia-Kalaba framework was evaluated and compared against specified target modal frequency and mode shape quantities from the FE model. The outputted torsional spring stiffnesses are presented in Table 6.

Table. 6 Solved torsional spring stiffnesses

Torsional spring stiffnesses, (4 decimal places)	
K_{T_1}	9.7957 x 10^3 Nmrad^{-1}
K_{T_2}	1.4624 x 10^7 Nmrad^{-1}

Validation of the obtained torsional spring stiffnesses was performed through re-incorporating the stiffness values within the Udwadia-Kalaba lumped parameter model of the inceptor control stick and numerically evaluating the system's numerical natural frequency. Comparisons were then made with the inceptor control stick's original modal frequency extracted from FEA. The modal frequency recorded from the FE model was 278.58 Hz. The numerical modal frequency obtained from the Udwadia-Kalaba lumped parameter model was found to be 278.55 Hz, constituting a 0.01% difference. The value of the MAC correlation between the numerically obtained mode shape with that of the original inceptor control stick was found to be 0.97089. The results reveal a strong matching of modal frequencies and respective correlation of mode shape data. The results show that the dynamic behaviour of the inceptor control stick

is represented with sufficient accuracy using the lumped parameter approach within the Udwadia-Kalaba framework. The remainder of the inceptor mechanism is now modelled and integrated with the lumped parameter model of the inceptor control stick.

C. Inceptor mechanism- Static model

The components of the inceptor mechanism deemed of interest as set out in Fig. 12 were discretised into a series of individual bodies. Geometric constraint equations governing each body's centre of gravity kinematic relations and configuration in three-dimensional space relative to the global coordinate frame of reference were derived. To effectively validate the derived system's geometric constraint equations and to determine initial and compatible starting value combinations of state variables for the mechanism dynamic model, the inceptor mechanism's static responses based on the derived constraint equations were firstly numerically modelled and solved for.

Static responses were then compared with results from an additional inceptor mechanism model produced within MATLAB's Simscape and from data provided by the inceptor manufacturer for validation. The inceptor's control stick angle was selected as the user-varied parameter. The quantity measured for static analysis is the ratio of the inceptor control stick angle variation with the rotation in the servo actuator gearbox shaft. The results of this static analysis is presented in Fig. 15.
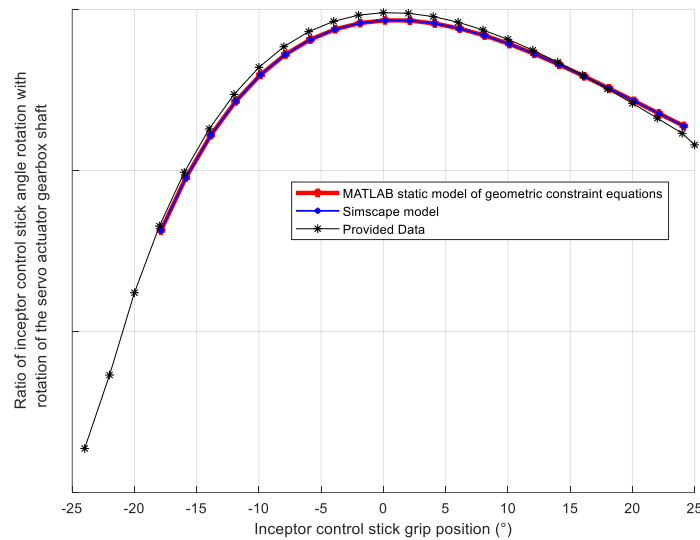

Fig. 15 Inceptor mechanism static responses.

Results from Fig. 15 show that static responses obtained from modelling the inceptor mechanism's derived geometric constraint equations directly match those produced from the alternatively formulated Simscape model. This observation provides verification to the derived system of geometric constraint equations of the inceptor mechanism. The slight variations observed between data provided by the inceptor manufacturer and responses obtained from modelling the inceptor mechanism's geometric constraint equations and Simscape model are primarily due to the assumed geometrical simplifications when discretising the inceptor system into a series of individual bodies. However, since the underlying trend of static responses from modelling the mechanism's geometric constraint equations closely agree with the provided data, the inceptor mechanism's derived geometric constraint equations are effectively validated. Results from Fig. 15 also reveal the nonlinear nature of the inceptor mechanism with clear nonlinear variations in the ratio of rotations of the inceptor control stick angle with servo actuator gearbox shaft.

D. Inceptor mechanism- Dynamic model

Upon determining initial and compatible starting values for state variables associated with the inceptor mechanism, dynamic modelling of the inceptor mechanism was conducted through the Udwadia-Kalaba approach. The system's natural frequencies and modes shapes were numerically evaluated. The frequencies numerically obtained are displayed in Table. 7.

Table. 7 Modal frequencies of the flexible nonlinear inceptor mechanism model

Mode	Modal frequencies of the U-K inceptor mechanism model, Hz
1	22.09
2	107.61

Results from the evaluation of the numerical natural frequencies of the inceptor mechanism with the inclusion of the control stick modelled through the lumped parameter approach reveal the presence of two modal frequencies as shown in Table. 7. The inceptor mechanism's first vibration mode recorded at 22.09 Hz is associated with the system's rigid body mode that corresponds to the fore-aft rocking motion of the control stick and connecting components. Results from the inceptor system unit FE model not discussed within this paper also concur. Additionally, an inspection of the inceptor mechanism's numerically obtained mode shape associated with the three rigid elements that represent the inceptor control stick support this observation. In Fig. 16a), the centre of gravity (CG) displacements of rigid elements 2 and 3 in the global Y-axis directions are in phase. However, the CG Y-axis displacement of rigid element 1 is in the opposite sense as expected due to its location on the opposite side of the control stick pivot as in Fig. 16b).
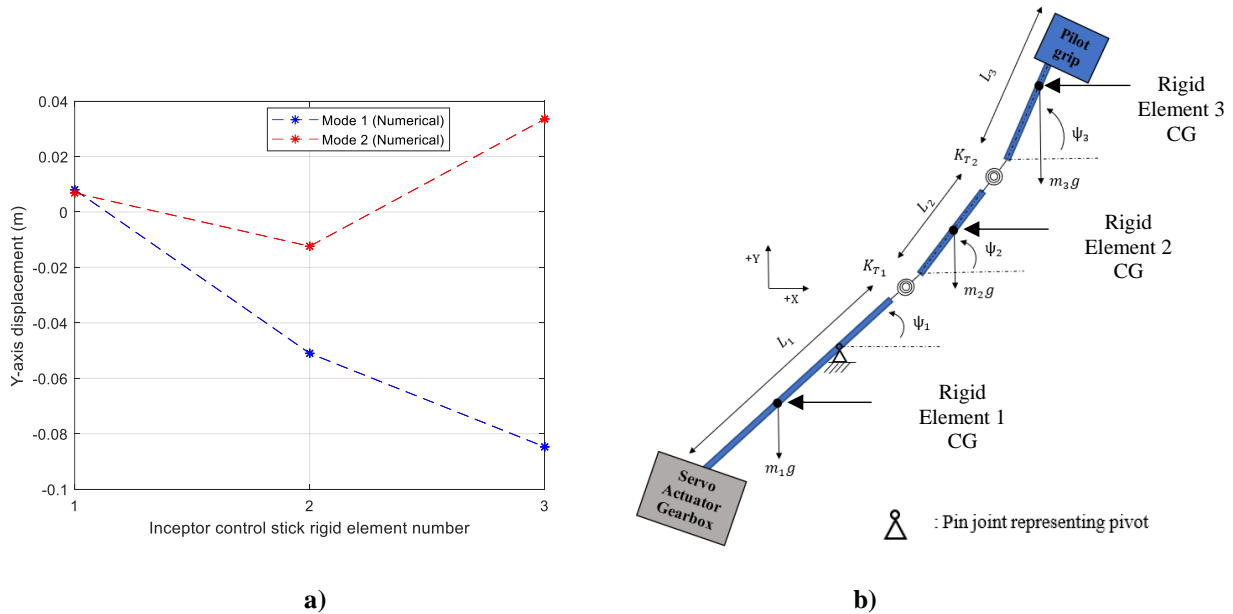

a) **b)**

Fig. 16 a) Numerically obtained mode shapes of the three rigid elements that represent the inceptor control stick b) lumped parameter model representation of the inceptor control stick.

The system modal frequency recorded at 107.61 Hz corresponds to the flexible fore-aft bending flexible mode of the inceptor control stick previously identified. The evaluation of numerical natural frequencies show a 61.37% reduction in the control stick's flexible modal frequency when it is constrained at its pivot and the remainder of the inceptor

17

mechanism incorporated. The observation of the system's numerically obtained mode shape in Fig. 16a) is also indicative of the presence of a flexible mode due to the opposing displacement directions of the inceptor control stick's rigid elements 2 and 3.

E. Inceptor mechanism- Tuning study

A series of tuning studies are now performed to demonstrate how the derived mathematical model of the inceptor system formulated using the Udwadia-Kalaba modelling approach may be used to tune system natural frequencies and offer parametric design insight. Through the specification of target frequencies and parameters designated for tuning, the capabilities of the mathematical model to inform and suggest modifications in the selected system design parameters to achieve the specified frequency levels are showcased. Three tuning studies will now be presented, the first and third requiring a reduction in inceptor mechanism frequencies with the second requiring inceptor mechanism frequencies to be increased.

In all cases two target inceptor mechanism frequencies are specified hence only two design parameters within the inceptor mechanism are considered for modification to satisfy the desired frequency targets. The backwards process outlined in Section IV was used which involved evaluating the numerical natural frequencies of the inceptor mechanism lumped parameter model formulated within the Udwadia-Kalaba framework and comparing quantities against specified target modal frequencies. The design parameters considered in the first two tuning studies are listed below and highlighted in red in Fig. 17a):

- Stiffness of the first torsional spring within the inceptor control stick lumped parameter model, (K_{T_1})

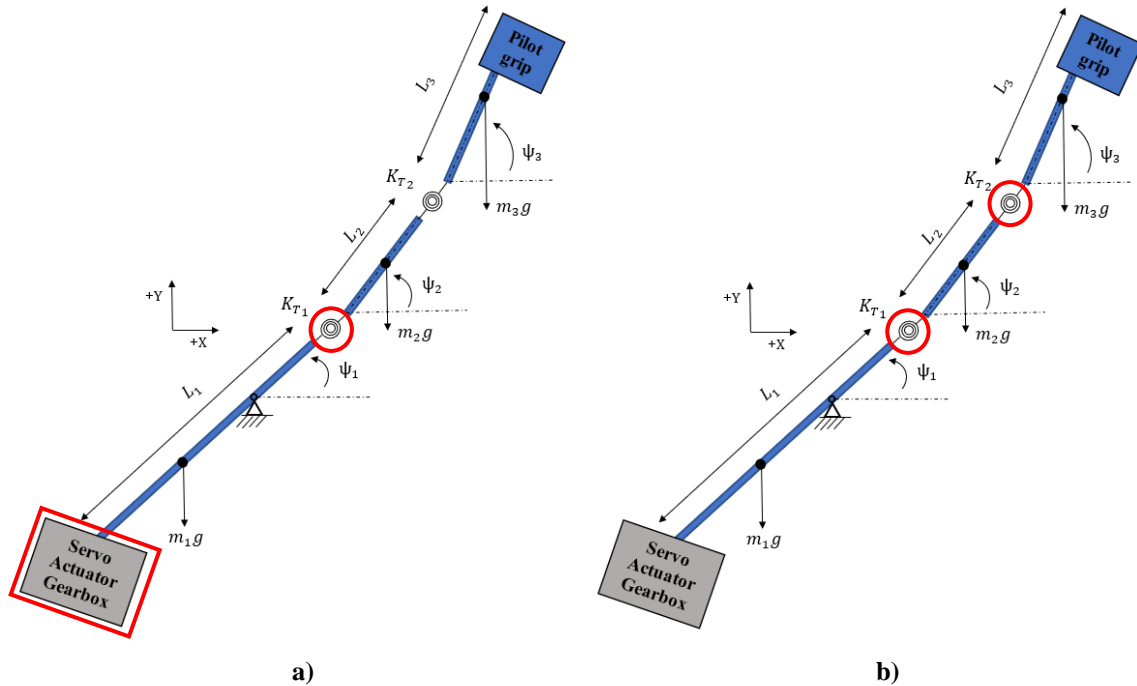- Servo actuator gearbox mass, (M_{SAU})

Fig. 17 Inceptor mechanism parameters considered for tuning highlighted in red
a) for tuning studies 1 and 2, b) for tuning study 3

The mass of the servo actuator gearbox was considered due to it's highest weight contribution to the inceptor mechanism. The stiffness of the first torsional spring within the lumped parameter inceptor control stick model was also considered to include the prospect of redesigning the physical inceptor control stick to meet the frequency level criteria.

For the third tuning study, only parameters associated with the inceptor control stick are considered. This is to include circumstances where the inceptor control stick is redesigned independently from the remainder of the mechanism. Specifically, the parameters considered are the stiffnesses of the two torsional springs within the inceptor control stick lumped parameter model (K_{T_1}, K_{T_2}) as highlighted in red in Fig. 17b)

3. Tuning study 1: Reduction in inceptor mechanism natural frequencies

For demonstrative purposes, the inceptor mechanism's natural frequency desired levels are set at 18 and 90 Hz. As illustrated in Fig. 18a) this constitutes a 18.52% reduction in the mechanism's first modal frequency and a 16.37% reduction the mechanism's second modal frequency.
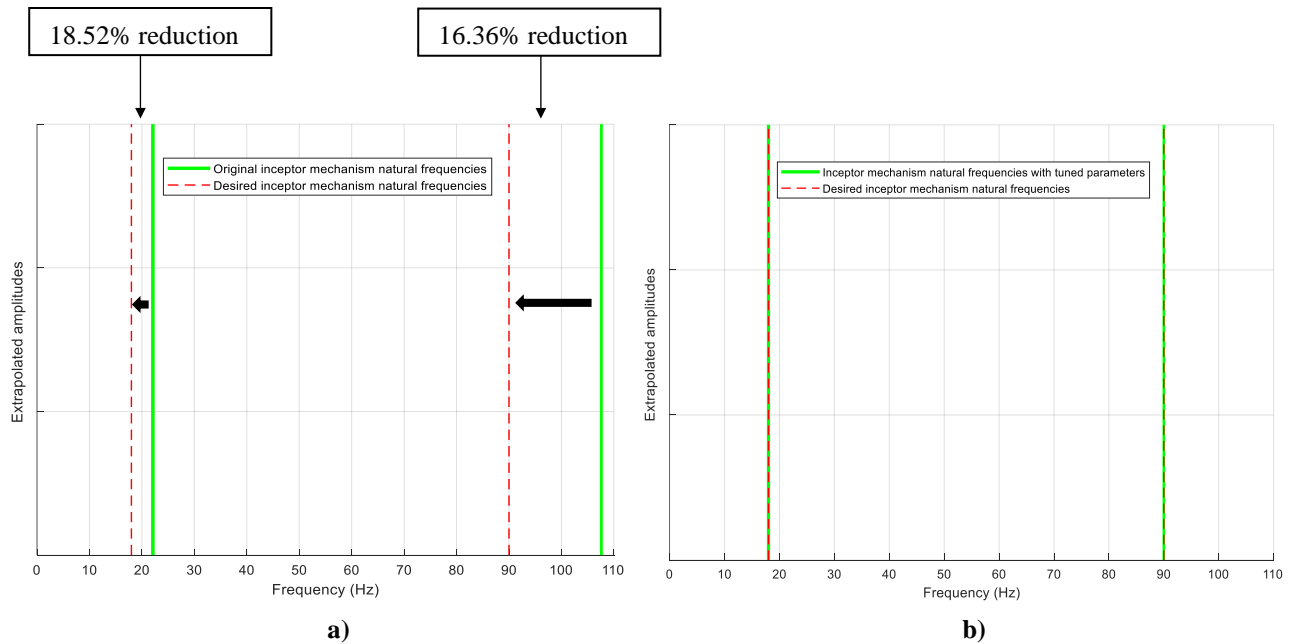
Fig. 18 a) Inceptor mechanism original natural frequencies and desired target levels
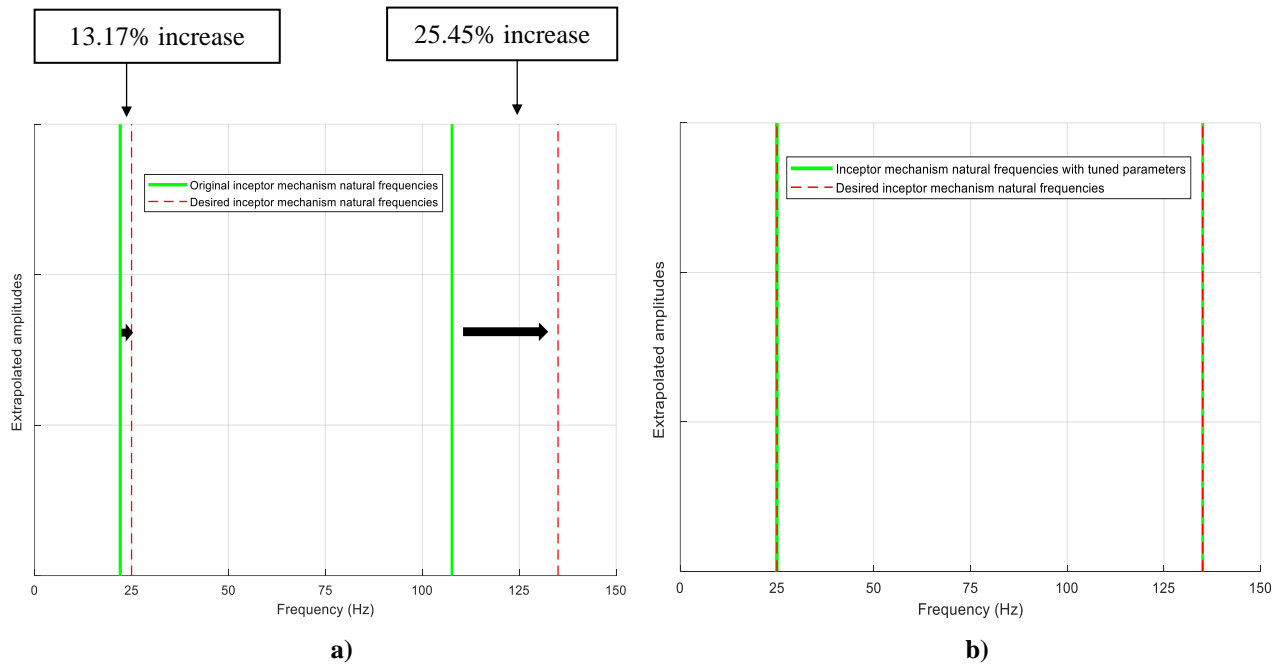**b) Inceptor mechanism natural frequencies with tuned parameters**

Table. 8 Tuning study summary for the selected inceptor mechanism parameters.

Inceptor mechanism parameter	Original values (4 decimal places)	Tuned values (4 decimal places)	Percentage change
M_{SAU}	2.2635 kg	6.0170 kg	+165.83 %
K_{T_1}	9.7957 x 10^3 Nmrad^{-1}	1.0147 x 10^4 Nmrad^{-1}	+3.59 %

Results from Fig. 18 show that the mathematical inceptor model may be used to tune inceptor mechanism natural frequencies to desired levels by recommending modifications to the selected inceptor mechanism design parameters. The mathematical model recommends increasing the values of both servo actuator gearbox mass and stiffness of the first torsional spring within the inceptor control stick model as an option for achieving the target frequencies as shown in Table. 8. It is suggested that the value of the servo actuator gearbox mass be substantially increased by 165.83% whilst the stiffness of the first torsional spring within the inceptor control stick model increase by 3.59% in comparison. By adopting these two tuned parameters, the resulting inceptor mechanism natural frequencies are found to now occur at the desired target frequency levels, thereby satisfying this tuning study as shown in Fig. 18b).

4. Tuning study 2: Increase in inceptor mechanism natural frequencies

For demonstrative purposes, the inceptor mechanism's natural frequency desired levels are now set at 25 and 135 Hz. This reflects to a 13.17% increase in the mechanism's first modal frequency and a 25.45% increase in the mechanism's second modal frequency.

**Fig. 19 a) Inceptor mechanism original natural frequencies and desired target levels
b) Inceptor mechanism natural frequencies with tuned parameters**
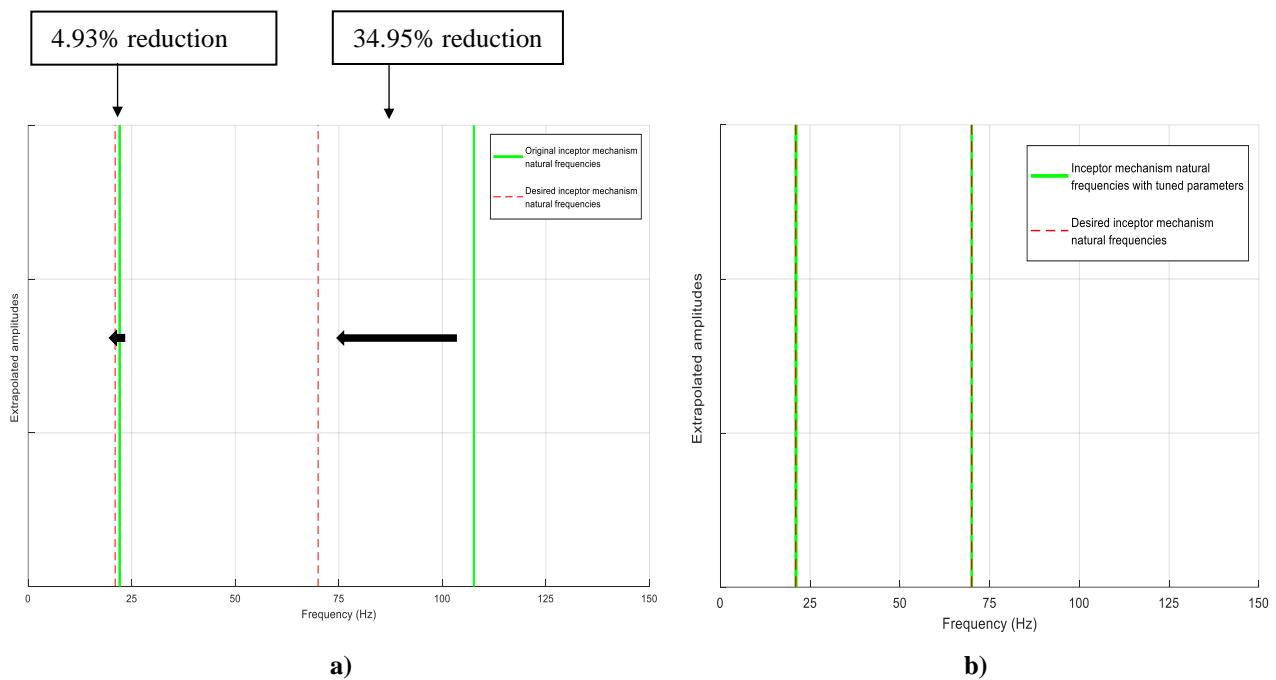
Table. 9 Tuning study summary for the selected inceptor mechanism parameters.

Inceptor mechanism parameter	Original values (4 decimal places)	Tuned values (4 decimal places)	Percentage change
M_{SAU}	2.2635 kg	0.4561 kg	-79.85 %
K_{T_1}	9.7957 x 10^3 Nmrad^{-1}	8.0219 x 10^3 Nmrad^{-1}	-18.11 %

Results from the mathematical model recommend a reduction in the two considered parameter values as an option to achieving the desired target frequencies as shown in Table. 9. It is suggested that the value of the servo actuator gearbox mass be substantially reduced by 79.85% whilst the stiffness of the first torsional spring within the inceptor control stick model reduce by 18.11 %. By updating these two parameters with their tuned values, the resulting inceptor mechanism natural frequencies now occur at the desired target frequency levels, thereby satisfying the frequency tuning study as shown in Fig. 19b).

5. Tuning study 3: Reduction in inceptor mechanism natural frequencies

For this tuning study, the inceptor mechanism's natural frequency desired levels are set at 21 and 70 Hz. This corresponds to a 4.93% reduction in the mechanism's first modal frequency and 34.95% reduction in the mechanism's second modal frequency as shown in Fig. 20a).

Fig. 20 a) Inceptor mechanism original natural frequencies and desired target levels
b) Inceptor mechanism natural frequencies with tuned parameters

Table. 10 Tuning study summary for the selected inceptor mechanism parameters.

Inceptor mechanism parameter	Original values (4 decimal places)	Tuned values (4 decimal places)	Percentage change
K_{T_1}	9.7957 x 10^3 Nmrad^{-1}	3.7684 x 10^3 Nmrad^{-1}	-61.53 %
K_{T_2}	1.4624 x 10^7 Nmrad^{-1}	1.4625 x 10^7 Nmrad^{-1}	+0.0002271 %

Results from the mathematical model show that stiffnesses of the two torsional springs within the inceptor control stick lumped parameter model may be tuned to achieve the desired inceptor mechanism natural frequencies. It is suggested that the stiffness of the first torsional spring (K_{T_1}) be significantly reduced, by 61.53% as seen in Table. 10.

It is also suggested that the stiffness of the second torsional spring (K_{T_2}) be increased. However, from the percentage change quantities, this recommended change in K_{T_2} is marginal in comparison. The results also provide insight into the parametric design and resulting behaviour of the inceptor mechanism. The extent to which the value of K_{T_1} is suggested to change coupled with the apparent invariant change in K_{T_2} to achieve the desired target frequencies highlights the dominance of K_{T_1} in influencing the natural frequencies of the two modes in consideration. If limitations are placed on the scope by which the parameter K_{T_1} may vary, results suggest that the second design parameter to tune ideally originate from components within the remaining inceptor mechanism to achieve the desired target frequencies. Nonetheless, by updating K_{T_1} and K_{T_2} with their tuned values in Table. 10, the resulting inceptor mechanism natural frequencies now occur at the desired target frequency levels, as shown in Fig. 20b). To the authors' knowledge, this is a unique approach to the mathematical modelling of an inceptor mechanism aimed at providing insight in the early design stage.

VI. Conclusion

The development of an efficiently configurable and *reduced-order* mathematical model of an active inceptor is desirable in providing an early low-cost means of predicting the dynamics of an inceptor mechanism at early design stages. The criteria for the model would be for it to be sufficiently tuneable and representative in order for it to be used to aid early design process stages by identifying acceptable inceptor design configurations that conform to frequency avoidance restrictions.

Dynamic analysis of a test case in the form of a flexible beam with varying root and end boundary conditions demonstrated the adaptation and applicability of using the lumped parameter approach within the Udwadia-Kalaba modelling framework to successfully represent the dynamic behaviour of the original system and predict it's natural frequencies. An iterative backwards methodology for obtaining the discretised model's lumped parameters within the Udwadia-Kalaba framework was also derived.

A flexible model of the candidate inceptor mechanism was derived by incorporating linkage flexibility within the control stick due to its geometry and inherent flexibility. The flexibility is idealised through lumped parameters within the Udwadia-Kalaba framework which has been shown to be applicable for generic multibody systems subjected to kinematical constraints.

Dynamic analysis of the inceptor mechanism using the lumped parameter approach within the Udwadia-Kalaba framework adequately predicted the locations and presence of the mechanism's natural frequencies that included flexible modes.

A series of tuning studies was also conducted to demonstrate how the derived mathematical model of the inceptor mechanism using the Udwadia-Kalaba lumped parameter approach may be used to tune system natural frequencies to desired levels by recommending modifications in selected system design parameters to achieve the desired frequency levels. The model has shown to be capable of also offering parametric design insight at early design stages.

The application of the Udwadia-Kalaba modelling approach to an inceptor mechanism and the demonstration of its ability to contribute to preliminary design studies is, to the authors' knowledge, a new contribution to the field. Future research efforts will build on the inceptor mechanism mathematical model by focusing on incorporating capabilities for lateral flexible modes of the control stick to be captured. Work will also be directed at improving the idealisation of inceptor control stick using the lumped parameter approach by representing it with an increasing number of elements. Eventually, efforts will lead to the cross comparison and subsequent tuning of numerical results with frequency responses obtained from experimental vibration surveys conducted on the physical inceptor. This will provide validity to the growing mathematical inceptor mechanism model of increasing complexity.

References

[1] Anon. *Active Inceptor Systems,* BAE Systems. http://www.baesystems-ps.com/pdf/ais_mil_brochure.pdf, [retrieved 17 November 2020]

[2] Anon. Air France flight AF 447 Rio de Janeiro-Paris Final Report, 2012, BEA, https://www.bea.aero/docspa/2009/f-cp090601.en/pdf/f-cp090601.en.pdf, [retrieved 29 November 2020]

[3] Anon. *Pilot controls- active sticks*, BAE Systems. https://baesystems-ps.com/pilot-controls.php, [retrieved 17 November 2020]

[4] Anon. *Aerospace Active Inceptor Systems for Aircraft Flight and Engine Controls,* Aerospace Recommended Practice (ARP) 5764, SAE International, 2013.

[5] Military Standard (MIL STD)- 810G, *Transportation Tailoring Guidance for Vibration Exposure Definition*, Method 514.6, Annex C, 317-318, 2008.

[6] Howell, L.L, Magleby, S.P, Olsen, B.M, *Handbook of Compliant Mechanisms,* John Wiley & Sons Ltd: Sussex, 2013, pp.31

[7] Yap, E.J.H., Rezgui, D., Lowenberg, M.H., Neild, S.A. & Rahman, K., "Resonant Frequency Tuning of a Nonlinear Helicopter Inceptor Model: A Sensitivity,". in: *Proceedings of the 45th European Rotorcraft Forum*., Warsaw, Poland, pp. 1-14, 2019

[8] Udwadia, F.E and Kalaba, R.E, *Analytical Dynamics A New Approach*, Cambridge University Press: Cambridge,1996.

[9] Bauchau, O.A, *Flexible Multibody Dynamics*, Springer, 2011, pp. 445-446

[10] Udwadia, F.E, Phohomsiri, P, "Explicit Poincaré equations of motion for general constrained systems. Part I. Analytical results"*Proceedings of the Royal Society A: Mathematical, Physical and Engineering Science*, Vol. 463, 2007

[11] Adams, The Multibody Dynamics Simulation Solution, https://www.mscsoftware.com/product/adams [retrieved 17 November 2020]

[12] DymoreSolutions, http://www.dymoresolutions.com [retrieved 17 November 2020]

[13] Moore-Penrose pseudoinverse documentation, MathWorks, https://www.mathworks.com/help/matlab/ref/pinv.html [retrieved 5 June 2020].

[14] Nielsen, M.C., Eidsvik, O.A., Blanke, M., Schjølberg, I., "Validation of Multi-Body Modelling Methodology for Reconfigurable Underwater Robots," Presented in the *OCEANS 2016 MTS/IEEE Monterey conference*, IEEE, Sept, 2016.

[15] Li, C., Zhao, H., Zhen, S., Sun, H., Shao, K., "Udwadia Kalaba theory for the control of bulldozer link lever," *Advances in Mechanical Engineering*, vol. 10, iss. 6, 2018

[16] Y. Xu, R. Liu, *Dynamic modeling of SCARA robot based on Udwadia-Kalaba theory,* Advances in Mechanical Engineering, Vol. 9(10), pp1-12, 2017

[17] Simscape documentation, MathWorks ver. 2020b, https://uk.mathworks.com/products/simscape.html, [retrieved 17 November 2020]

[18] Patran, Complete FEA Modeling Solution, https://www.mscsoftware.com/product/patran [retrieved 17 November 2020]

[19] Fsolve documentation, MathWorks ver.2020b, https://uk.mathworks.com/help/optim/ug/fsolve.html [retrieved 24 November 2020]

[20] Numjac documentation, https://www.mathworks.com/matlabcentral/mlc-downloads/downloads/submissions/47171/versions/1/previews/A3_Distill/numjac.m/index.html [retrieved 24 November 2020]

[21] Ewins. D. J, *Modal Testing theory, practice and application.* 2nd Edition, Research Studies Press Ltd, Hertfordshire, 2000.